Review

Acoustic wave biosensors: physical models and biological applications of quartz crystal microbalance

Guilherme N.M. Ferreira[1], Ana-Carina da-Silva and Brigitte Tomé

IBB-Institute for Biotechnology and Bioengineering, Centre for Molecular and Structural Biomedicine, University of Algarve 8005-149 Faro

Piezoelectric sensors are acoustic sensors that enable the selective and label-free detection of biological events in real time. These sensors generate acoustic waves and utilize measurements of the variation of the wave propagation properties as a signal for probing events at the sensor surface. Quartz crystal microbalance (QCM) devices, the most widespread acoustic resonators, allow the study of viscoelastic properties of matter, the adsorption of molecules, or the motility of living cells. In a tutorial-like approach, this review addresses the physical principles associated with the QCM, as well as the origin and effects of major interfering phenomena. Special attention is paid to the possibilities offered by QCM that go beyond microweighing, and important recent examples are presented.

Introduction

The integration of advanced microelectronics technology with signal processing and biological sensing interfaces, with the aim of generating biosensor devices, has emerged as a rapidly growing area of enormous potential. The field of biomolecular sensors is now beginning to emerge as a valuable tool for understanding the underlying biophysical principles of molecular recognition, as well as detecting the presence of specific analytes. The 'holy grail' of biosensors is the development of rapid, simple, selective and label-free detection methodologies to measure and transduce the biological events that occur in a particular setting. Currently available biosensors have already been used widely in clinical diagnosis, biomedicine, environmental monitoring and pollution control, military and security applications, as well as in food safety and industrial applications [1].

The International Union of Pure and Applied Chemistry (IUPAC) definition of a biosensor is given as 'a biosensor is a self-contained integrated device that provides quantitative analytical information using a biological recognition element retained in direct contact with a physical transduction element'. The biological recognition element (e.g. bioreceptors, antibodies, DNA, enzymes, or cells) guarantees the selective recognition of target analytes, whereas the transducer converts binding events into a measurable electrical signal, which is correlated with the build-up of concentration, or the activity of the analyte in the vicinity of the device (Figure 1).The use of acoustic waves is one of the most appropriate direct transduction mechanisms, because the parameters that describe the wave propagation (e.g. wave velocity) depend on the properties of the propagating material (see below). While acoustic waves can be generated by several means, the piezoelectric effect has been employed most widely, both to generate and to receive acoustic waves [1–4]. Piezoelectricity is associated with the reversible polarization of certain materials and is produced by mechanical strain. This phenomenon was initially described by the Curie brothers and has been used extensively to promote the propagation of transverse acoustic waves across the bulk of appropriate crystalline materials (Figure 2a). Piezoelectric transduction enables a label-free detection of biorecognition events and typically is used in microgravimetric devices, generally known as quartz crystal microbalance (QCM), in a variety of different applications, such as monitoring and characterization of (bio)film deposition, detection of specific antigens, biomolecule binding kinetics, cell adhesion, and DNA detection [1,5–11].

This review describes the theoretical aspects of QCM operation in liquid environments. Particular emphasis is placed on the tutorial description of the physics that underlie the signal generation. This aims to provide a broad and comprehensive understanding of the role of the most relevant parameters associated with the sensor–liquid interphase, which might cause or potentiate interference in the signal, as well of different approaches for measuring and examples of applications.

Fundamental aspects of quartz crystal sensors

A QCM is a thickness shear mode (TSM) acoustic wave resonator, in which an AT-cut thin quartz disk (i.e. a disk cut from a quartz mineral at a 35.25° orientation to its optical axis) is sandwiched between two metal electrodes, typically made of gold. As a result of the piezoelectric nature of the quartz material, the application of an alternating electric field produces a shear (tangential) deformation. Upon deformation, both surfaces move in parallel but opposite directions, being thus motion antinodes, thereby generating acoustic waves that propagate through the bulk of the material across the crystal, in a direction that is perpendicular to the surface, and with wavelengths that are multiple factors of double the thickness of the substrate (t_Q) (see Figure 2a). In fact, upon reflection at each of the sensor surfaces, a constructive interference between

Corresponding author: Ferreira, G.N.M. (gferrei@ualg.pt)
[1] Current address: Department of Physics, University of California Santa Barbara, Santa Barbara CA 9316, California, USA..

0167-7799/$ – see front matter doi:10.1016/j.tibtech.2009.09.003 Available online 23 October 2009

incident and return acoustic waves occurs when the wavelength is an odd multiple of the double substrate thickness, and hence, standing wave conditions are established [4]. The resonance frequency, also termed eigen frequency (f) of the crystal, depends on the shear acoustic wave velocity (ν) and the thickness of the crystal substrate, and can be expressed as: $f = n \times \nu / 2t_Q$, where n is the overtone. The fundamental resonance frequency (f_0) is obtained for n=1 and only odd overtones (n = 1,3,5,...) can be excited, as predicted by the acoustic wave propagation equation [4,12]. Moreover, as the shear acoustic wave velocity (ν) is highly dependent on the properties of the propagating materials (i.e. $\nu = (E/\rho)^{1/2}$, where E is the stiffness (Young modulus) and ρ the density, TSM resonators are able to determine material-specific parameters, which are not easily obtained, or even impossible to obtain using other biosensors with direct transduction, such as optical sensors based on surface plasmon resonance (SPR) [4].

By relating the mass of the crystal material with its density (i.e. $m = A \times t_Q \times \rho$, with A being the area) it is possible to predict the resonant frequency variation that is associated with small mass increases (ΔM) at the surface of the sensor, according to Equation 1:

$$\Delta f_0 = -\frac{2}{\sqrt{E\rho}} f_0^2 \times \frac{\Delta M}{A} \qquad \text{(Equation 1)}$$

This equation is the so-called Sauerbrey equation [13], which establishes a linear relationship between resonant frequency and small mass increments. The Sauerbrey equation makes the assumption that the mass deposited, or the film formed, at the surface of the crystal follows the vibration of the crystal and therefore the loaded crystal would simply behave as if it were thicker. The effective wavelength of the crystal is thus increased and consequently its resonant frequency decreases. This model assumes that no energy dissipation occurs and will thus only be valid for thin, rigid and uniform films that have similar acoustic properties as those of the bulk crystal material [4].

However, when the resonator becomes immersed in a fluid, as required for biosensing applications, or the acoustic properties of the added viscoelastic probe layer differ significantly from those of the crystal sensor, energy is lost to the fluid through so-called viscous coupling [4,14], as the shear acoustic waves are transmitted to the fluid, which results in a velocity profile that is described by the Navier–Stokes equation for one-dimensional plane parallel flow [4,12,14,15] (see Figure 2b).

The effect of viscous coupling was modelled by Kanazawa and Gordon [16,17], who solved the simultaneous wave propagation and the Navier–Stokes equations by assuming that no slip occurs at the solid–liquid interface, that is, the fluid near the surface moves at the same velocity as the surface. The resulting solution predicts a decrease in sensor resonant frequency, owing to liquid damping that is proportional to the viscosity (η_L) and density (ρ_L) of the fluid (see Equation 2), and that a transverse shear wave propagates into the fluid that dissipates exponentially with a decay characteristic length (δ) that depends on the resonant frequency (Equation 3).

$$\Delta f = -f_0^{3/2} \sqrt{\frac{\rho_L \eta_L}{\pi E \rho}} \qquad \text{(Equation 2)}$$

$$\delta = \sqrt{\frac{2\eta_L}{\omega \rho_L}}, \qquad \text{(Equation 3)}$$

were $\omega = 2\pi f$ if the angular frequency

Equation 3 shows that the acoustic shear wave that is transmitted into the fluid propagates to a greater extent (higher decay length) into fluids with higher kinematic

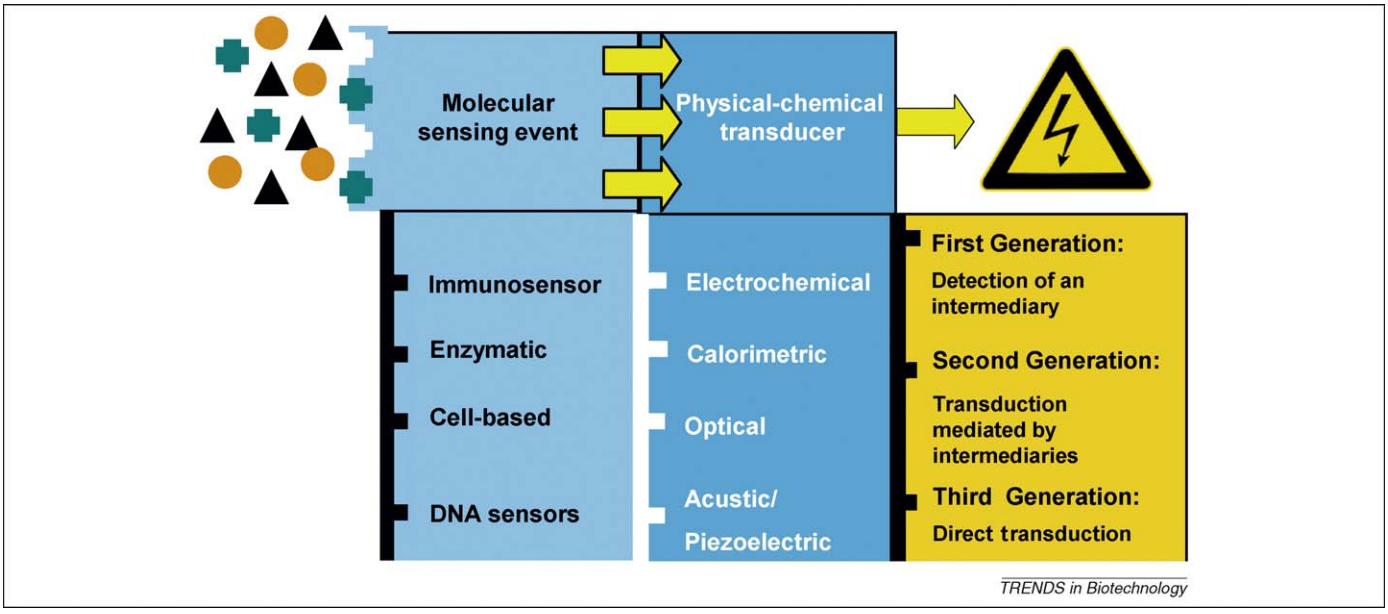

Figure 1. Schematic illustration of a Biosensor. A biosensor is an integrated device that contains a molecular sensing layer that is directly attached to a physicochemical transduction element. The molecular sensing layer ensures the recognition of specific targets, while the transduction element converts binding events into an electrical signal, the intensity of which is correlated with the concentration or activity of the target analytes. Biosensors are classified according to the mechanisms by which biological specificity is conferred and the mode of physicochemical signal transduction. For instance, optical immunosensors or electrochemical DNA sensors are defined as biosensors with immobilized antibodies and optical transduction, or as immobilized DNA strands with electrochemical detection, respectively. With regard to their signal generating method, biosensors are designated as first-, second-, or third-generation devices depending on whether an intermediary is detected, the dection is mediated by an intermediary, or the specific target is detected directly (so-called direct transduction).

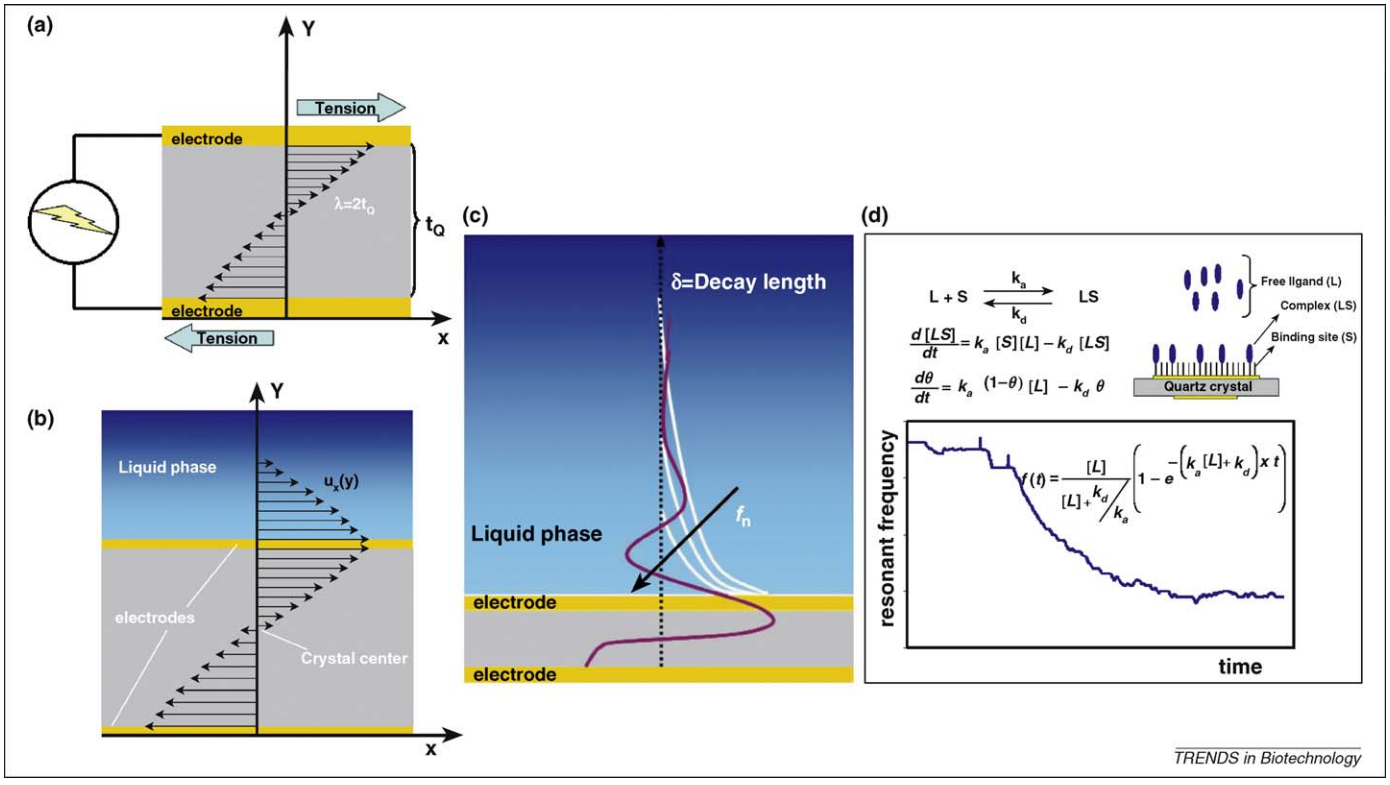

Figure 2. Fundamental aspects of quartz crystal sensors. **(a)** The application of an electric field produces tangential deformation that results in an acoustic wave that propagates across the crystal material. **(b)** If the sensor is immersed in a fluid, the acoustic wave is propagated into the fluid, which results in a one-dimensional plane-parallel flow velocity profile. **(c)** The amplitude (white lines) and decay length (δ) of the acoustic wave transmited to the fluids (purple line) decrease with increasing sensor resonance frequency, or overtone (f_n). **(d)** Example of use of QCM to estimate binding constants. The sensor resonance frequency variation is monitored continuously and the Sauerbrey equation is used to establish a direct relationship between the resonance frequency and the mass or concentration of ligand (*L*) bound to the surface binding sites (S), therefore providing an estimate of the ligand surface coverage (θ). As θ is proportional to the frequency variation *f*(t), the integrated rate equation (inset equation) is fitted to the experimental frequency variation data measured at different concentrations of ligand (*L*). The kinetic binding constants (k_a and k_d) are then calculated from a linear correlataion of each one of the obtained exponantial terms and the respective ligand concentration (*L*).

viscosity (η_L/ρ_L). Quartz crystal resonators only respond to the fluid that is present in regions very near to the sensor surface; for instance, Equation 3 predicts a penetration depth (decay length) of 250 nm for a shear acoustic wave propagating in water and generated from a 5-MHz crystal microbalance. Another important outcome of Equation 3, with far-reaching practical consequences, is the dependence of the decay length on the sensor resonance frequency, which enables probing at different distances from the sensor surface, which allows one to obtain information about different layers upon measuring at the sensor overtones (Figure 2c).

The immediate outcome of Equations 1–3 is that QCM will respond to mass deposition and liquid loading. In addition, as the frequency change is affected significantly by the density and viscosity of the liquid, QCM will also respond to differences in the viscosity of the buffer and injected samples, as well as to viscosity changes arising from variation in temperature.

Martin and co-workers [14] have derived a model for the total frequency change that accounts for the simultaneous contribution of mass and liquid loading to the sensor signal (Equation 4):

$$\Delta f = \Delta f_m + \Delta f_L = -\frac{2 f_0^2}{n(C_{66}\rho_q)^{1/2}}\left[\frac{\Delta m}{A} + \left(\frac{\rho_L \eta_L}{4\pi . f_0}\right)^{1/2}\right] \qquad \text{(Equation 4)}$$

where $C_{66} = 2.957\times10^{10}$ N.m^{-2} is the stiffness of quartz.

As a result of the additive nature of mass and liquid loading illustrated by Equation 4, the contribution of the mass increase cannot be differentiated from that of liquid loading when tracking the overall frequency change, and the obtained data need to be carefully evaluated and interpreted.

Despite this apparent disadvantage, QCM sensors can still be employed successfully using standard oscillator techniques and frequency counting, because they exhibit a number of advantages including low cost and simplicity of operation and data analysis. The sensor resonance frequency is monitored continuously and, upon sample application, the resonance frequency variation is further obtained by comparison with a reference. Typically, the Sauerbrey equation (Equation 1) is used to estimate the overall adsorbed mass, based on the total frequency variation obtained, or to establish a frequency variation (signal) to mass direct relationship, which is necessary to determine any binding kinetic constants from the frequency variation data [18] (Figure 2d). In this mode of operation (standard oscillation with resonance frequency counting), it is assumed that the use of reference measurements will eliminate most of the liquid loading effects, because these are considered to be equal in both the sample and the reference.

Deviations in the QCM response

Although the use of QCM as a transducer in the development of biosensing tools has exploited mainly the direct

relationship between mass and frequency, as described by the Sauerbrey equation (Equation 1), this approach generally is biased because viscoelastic effects (as described earlier) are not taken into consideration. This might result in misinterpretation of experimental data, and lead potentially to erroneous conclusions. This is particularly important in life sciences, where the use of biomolecules requires handling the sensors and measuring the signal in complex liquid buffers. In addition, biomolecules also commonly lead to considerable alterations of the viscoelastic properties near the sensor surface, which renders the signal from the sensor unsuitable to be interpreted under the ideal conditions that allow the use of the Sauerbrey equation.

The properties of the used liquids are however only one important factor that influences the response of the resonant frequency of a TSM. Variation in resonant frequency are also affected by changes in the roughness of the sensor surface [12,19,20], the solution permittivity and conductivity, as well as by the presence of charged species near the sensor surface [4,21–24]. Others factors are the viscoelastic properties of the adsorbed films and the occurrence of compressional waves [25–31].

Surface uniformity is of particular relevance because it is one of the conditions under which the Sauerbrey model can be used reliably to relate resonance frequency and deposited mass. In the case of a non-uniform surface, acoustic waves that are generated and reflected from the surface back into the crystal might have different amplitudes and therefore different wave vectors. This disrupts the establishment of positive interference, which occurs on ideal uniform surfaces, and result in energy dissipation and thus in variations in the sensor resonant frequencies [31].

However, a certain extent of surface roughness, either on the quartz crystal surface itself or on the adsorbed film, typically is inevitable, as are the interactions based on the wettability of the surface, that is, its degree of hydrophilicity or hydrophobicity. Surfaces that are rough or hydrophilic, tend to entrap liquids in their small cavities, therefore adding to the overall frequency variation observed, and subsequently, an increase in detected mass [4,20,32]. On the other hand, hydrophobic cavities on the surface are not wetted by the liquid, and instead, result in the inclusion of air or vacuum, which leads to reduced energy losses compared to those of hydrophilic surfaces [33]. The major consequence of this behaviour is the tendency of the resonance frequency variation to decrease with increasing hydrophobicity of the surface [4]. Additionally, with increased surface hydrophobicity, the fluid slip at the sensor surface also increases, and therefore, the 'no slip'-conditions, a prerequisite for the validity of the models mentioned earlier, are no longer valid. These phenomena are particularly relevant when biological molecules are used with QCM sensors, because the hydrophobic character of the surface might significantly change during biomolecule adsorption, owing mostly to the hydrophobicity of biomolecules, and thus result in a significant increase in dissipated energy, which in turn could lead to variations in the resonance frequency [34,35].

The use of conductive liquids, or of liquids with a high ionic strength and permittivity, also affects the resonant frequency of quartz crystals in solution, because these liquids can increase the piezoelectrically effective surface of the quartz crystal, even when the liquid is only in contact with the grounded electrode [36]. This effect is of particular importance for buffers with low ionic strength, because in this case, the parasitic frequency variation can be of the same order of magnitude as the measured signal [4,24]. The presence of charged species can additionally perturb the electrical double layer and also lead to significant frequency variations [22–24]. The electrical double layer was found to have a rigid structure [22,23], which, in accordance with Equation 1, is translated into resonant frequency variations in addition to those that are caused by mass deposition [22–24]. It is important to note that the influence of charged species and that of the electrical double layer is negligible when buffers with high ionic strengths ($I > 150$ mM) are used [24]. The use of buffers with high ionic strengths is thus a wise option to eliminate the influence of charged species [24].

Another effect that needs to be considered is the occurrence of liquid evaporation, which can lead to periodic changes in the resonance frequency in TSMs that have been submerged in open chambers [31]. As demonstrated by Martin and Hager [37], this behaviour can be explained by the generation of compressional waves as liquid evaporation changes the height of the air–liquid interface. This can result in positive or negative interference as the acoustic waves are reflected at the air–liquid interface [31,37]. This limitation can however be overcome with the use of a closed chamber [4,37].

Impedance analysis of QCM

The classical QCM operation based on the Sauerbrey equation allows one only to obtain the sensor resonance frequency and its variation as the sole experimental parameter. As described above, these measurements are biased because the resonance frequency is influenced by several factors that have to be accounted for to be able to quantify accurately analytes or kinetic data. Impedance analysis enables a full description of the acoustic load of the biosensor and thus makes it possible to identify and eliminate any interfering signals [14,15,38–44].

The impedance of the sensor is a complex vector quantity (Z=R+iX) that depends on the frequency of the applied signal. The imaginary terms of the complex impedance (X), termed reactance, represent energy storage, whereas, the real part of the impedance vector, the resistance (R), represent energy dissipation [3,4,14].

Physically, the impedance (Z) is the ratio between the applied voltage across the crystal and the current flowing through the crystal. In impedance analysis, the incident voltage versus the reflected sinusoidal voltage from the quartz crystal is measured within the resonant frequency, and the impedance magnitude and phase angle are calculated. The magnitude ($|Z|$) of the impedance provides a measure for the signal attenuation, whereas the phase (Θ_Z) measures the lag between the applied field and the resulting displacement [4]. As deducted in Box 1, the impedance of the sensor (Z) comprises an inductor (L_m), a resistor (R_m) and a capacitor (C_m), which arise from the inertia, damping and elastic stress terms, respectively [4,14,24]. Together,

these parameters define the motional arm of a Butterworth–van Dyke (BVD) model of a quartz resonator (Figure 3a), which includes an additional parallel capacitor (C_0) to account for the dielectric energy storage because the resonating crystal is situated in between two electrodes [38–44]. Table 1 summarizes the expressions of the BVD circuit parameters as they occur at the fundamental resonance of the sensor.

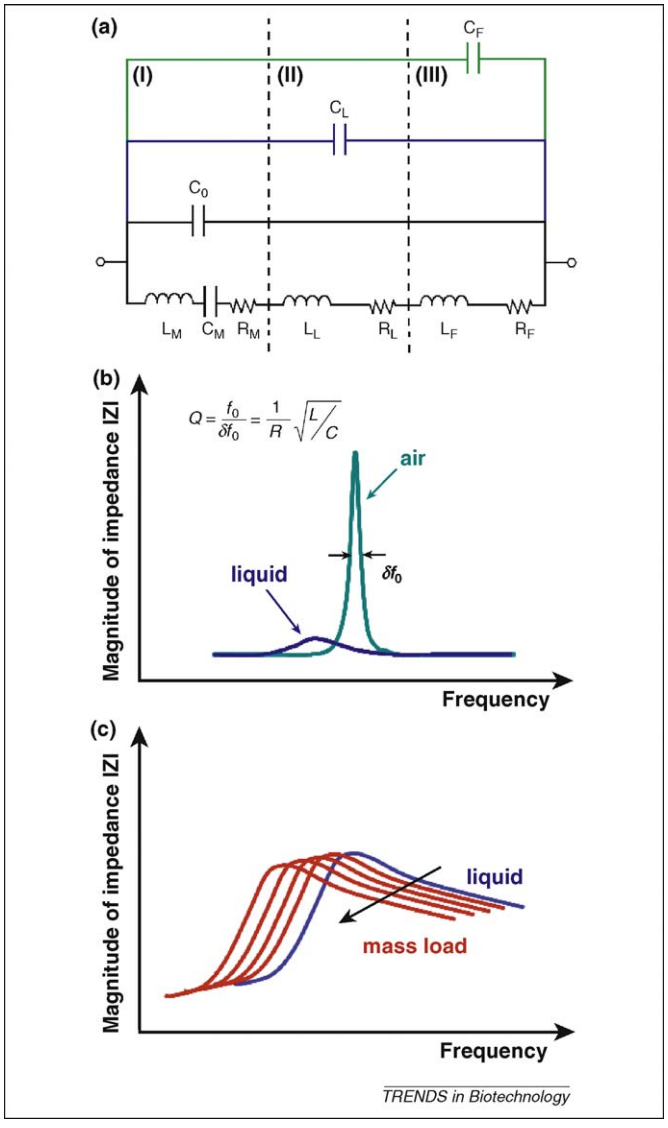

Figure 3. Impedance analysis of QCM. **(a)** Modified Butterworth-van Dyke equivalent electrical circuit (BVD) of a QCM sensor. Three circuits are shown that represent the sensor being exposed to air (black circuit, area I) or liquid (blue circuit), as well as the case of mass loading (green circuit). The BVD circuit for the sensor exposed to air (area I) comprises an inductor (L_M), a resistor (R_M) and a capacitor (C_M), which arise from the inertia, damping and elastic stress terms, in parallel with a capacitor (C_0) to account for dielectric energy storage. C_M is related to the overall sensor apparatus (mounting cell and cables), being thus constant. Each circuit is obtained by adding to that representing the sensor exposed to air (I), additional L, R, and C elements to account for variations in mass, viscoelasticity and charge upon liquid exposition (II) and/or upon mass adsorption (III), respectively. **(b)** Schematic illustration of the magnitude of the impedance for a QCM exposed to air and liquid. When the sensor is immersed in liquid buffer, the magnitude of its impedance is dampened considerably compared to that obtained in air. In additon, in liquids, its peak also shifts to lower frequencies, with decreased amplitude and broader shape. The quality factor (Q) can be calculated from the impedance curve as a parameter to quantify the dissipation. **(c)** Schematic illustration of the course of the sensor impedance variation upon mass adsorption at the QCM surface. As rigid mass adsorbs to the sensor surface, the impedence peak continuously shifts to lower frequencies. However, in contrast to immersion into liquids, where energy dissipation occurs, the width of the peak remains unchanged, which indicates that no additional energy dissipation occurs as expected for rigid mass adsorption.

Box 1. Derivation of the impedance of a QCM

The resonance of a QCM can be modelled as a damped oscillatory motion. The force balance of a vibrating mechanical structure that consists of a mass, a spring and damper is given by

$$F = m\frac{d^2x}{dt^2} + \eta\frac{dx}{dt} + kx$$

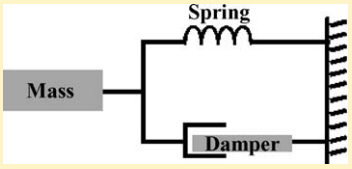

Solving the differential force equation using the Laplace transforms, dividing by the velocity (V), and using the transformed equation in the frequency domain $s = i\omega$ ($i = \sqrt{(-1)}$, ω being the angular frequency), an expression for a driving force divided by a flow like term (impedance) is obtained:

$$\frac{F}{V} = i\omega m + \frac{k}{i\omega} + \eta$$

This equation defines the impedance (Z) of the resonator. The three terms at the right hand side of this equation are equivalent to the impedances of an electrical inductor (L), a capacitor (C) and a resistor (R), respectively. These three electrical components are thus said to form the motional arm of an electrical equivalent circuit of the resonator. The impedance of the resonator is therefore a complex number whose representation in polar coordinates defines the impedance magnitude ($|Z|$) and phase (Θ_Z)

$$Z = |Z| \times e^{i\Theta_Z}$$

The condition for the circuit being in resonance implies that the imaginary part of the impedance is zero. Under these conditions, and if damping is negligible ($R_m \rightarrow 0$), the quartz resonator shows two resonance frequencies that correspond to a phase shift $\Theta_Z = 0$; the resonant frequency (f_R) at the minimum value of impedance and the antiresonant frequency (f_A) at maximum impedance magnitude [14,33,44]. On the other hand, if damping occurs ($R_m > 0$), four different resonant frequencies are discernable. At minimum impedance and at zero phase in the low-frequency branch, f_R separates into f_{Zmin} and f_s, the serial resonance frequency, whereas at maximum impedance and at zero phase in the high-frequency branch, f_A separates into f_{Zmax} and f_p, the parallel resonance frequency [44] (see also Table 1).

Figure 3 shows impedance simulations of a 5-MHz crystal resonator in air or immersed in a Newtonian liquid, and upon mass adsorption in liquid. Typically, immersing the sensor in liquid (as shown in Figure 3b) results in a shift of the resonance to lower frequencies, associated with a decrease and broadening of the impedance that arises from the energy dissipation associated with increasing R_m. Additionally, although the resonant and antiresonant frequencies are independent of R_m, the series and parallel resonant frequencies converge and eventually coincide [4]. The difference between f_{Zmin} and f_{Zmax} also increases, which reflects the broadening of the resonance peak [44].

On the other hand, as mentioned earlier, the deposition of rigid mass can be treated as an increase in the sensor thickness. The increase of vibrating mass is translated into increasing L_m, which is reflected by a shift of the resonance

Table 1. Impedance parameters of AT-cut crystal sensors[a]

Parameter	Expression	Description
R_m	$\frac{t_q \eta_q \pi^2}{8Ae_{26}^2}$	Oscillating energy dissipation into the structure onto which the crystal is mounted and into the medium (viscous solutions and viscoelastic films).
C_m	$\frac{8Ae_{26}^2}{\pi^2 t_q C_{66}}$	Stored energy in oscillation, which is related to crystal elasticity.
L_m	$\frac{t_q^3 \rho_q}{8Ae_{26}^2}$	Oscillation inertial component, which is related to the dislocated mass during vibration.
C_0	$\frac{\varepsilon_{22} A}{d_q}$	Static capacitance of the crystal electrodes, holding structure and cables.
f_R	$\frac{1}{2\pi}\sqrt{\frac{1}{L_m C_m}}$	Resonance frequency
f_A	$\frac{1}{2\pi}\sqrt{\frac{1}{L_m C_m}+\frac{1}{L_m C_0}}$	Anti-resonance frequency
f_s	$\frac{1}{2\pi}\sqrt{\frac{1}{L_m C_m}}\left(1+\frac{C_0 R_m^2}{2L_m}\right)$	Series resonance frequency
f_p	$\frac{1}{2\pi}\sqrt{\frac{1}{L_m C_m}}\left(1+\frac{C_m}{2C_0}-\frac{C_0 R_m^2}{2L_m}\right)$	Parallel resonance frequency
f_{Zmin}	$\frac{1}{2\pi}\sqrt{\frac{1}{L_m C_m}}\left(1-\frac{C_0 R_m^2}{2L_m}\right)$	Frequency at minimum impedance zero phase
f_{Zmax}	$\frac{1}{2\pi}\sqrt{\frac{1}{L_m C_m}}\left(1+\frac{C_m}{2C_0}+\frac{C_0 R_m^2}{2L_m}\right)$	Frequency at maximum impedance at zero phase

[a] A is the electrode area, η_q the viscosity, t_q the thickness, ρ_q the density, e_{26} the piezoelectric constant, ε_{22} the stiffened elasticity, and C_{66} is the permittivity of the AT-cut quartz material.

to lower frequencies while maintaining the magnitude of the impedance (Figure 3c). Nevertheless, if rigid mass is added, the separation between the frequencies f_{Zmax}, f_A, f_p, f_{Zmin}, f_R, and f_s is maintained, as an indication that no dissipation occurs [44]. It should be noted that in the oscillation mode of a TSM, only the serial resonance frequency can be measured, thus making it difficult to infer the occurrence or extent of energy dissipation.

The Q factor, the ratio between the height of the resonance peak and its width at half maximum, can also be obtained from impedance spectra (see Figure 3b). In physical terms, the Q factor represents the fraction between energy stored and energy lost in a single oscillation, and therefore, is a quantitative measure for energy dissipation. However, the most commonly determined parameter to account for dissipation in QCM experiments is the dissipation factor, which is defined as the reciprocal of the Q factor [4,12].

Applications in TSM biosensors

The different applications of acoustic sensors are all based on the same physical principle; the propagation of acoustic waves in a multilayer structure. The acoustic load impedance reflects these changes, irrespective of whether these are caused by mass accumulation, changes in the material properties (e.g. swelling, softening or rigidity), or chemical (e.g. cross-linking) and physical (e.g. phase transition) modifications. [40].

Under the conditions of low acoustic load [4,14,16,17], the impedance of the loaded sensor can be expressed as an additional element in series to the BVD equivalent circuit (Figure 3a). In Table 2, the impedance parameters for the three most relevant scenarios in biological applications are summarized. Under these conditions, the impedance of crystal loads by multiple layers can be described as linear combinations of the impedance of each one of the layers [16]. Thus, when liquid is added or mass is deposited on the crystal surface, new elements can be added to the BVD model to describe the overall impedance [45,46] (Figure 3a). This makes it possible to identify the effect of each of the layers simply by measuring the impedance in a step-wise manner as each component of the measuring sample (e.g. buffer, or target molecules) is added [14,16,17,31–34,41].

Table 2. Mathematical expressions of motional inductance (L_m) and resistance (R_m) for particular loads on AT-cut quartz resonators [3][a]

Load	L_m	R_m
Rigid mass	$\frac{n\pi}{4K^2\omega C_0}\frac{\rho_s}{Z_q}$	0
Newtonian liquid	$\frac{n\pi}{4K^2\omega C_0 Z_q}\sqrt{\frac{\rho_L \eta_L}{2\omega}}$	$\frac{n\pi}{4K^2\omega C_0 Z_q}\sqrt{\frac{\omega\rho_L\eta_L}{2}}$
Semi-infinite Viscoelastic layer	$\frac{n\pi}{4K^2\omega C_0 Z_q}\left(\frac{\rho(\lvert G\rvert - G')}{2}\right)^{1/2}$	$\frac{n\pi}{4K^2\omega C_0 Z_q}\left(\frac{\rho(\lvert G\rvert + G')}{2}\right)^{1/2}$

[a] K is the electroacoustic coupling factor, $Z_q = \sqrt{(\rho_q \mu_q)}$ is the acoustic impedance of the quartz; G is the complex shear modulus of the viscoelastic material; the real part is the storage modulus G' and the imaginary part is the loss modulus G''.

The most important objectives of biosensors are to quantify the amount of an analyte in a biological fluid, or to determine the kinetic constants for the binding of a biomolecule to a specific immobilized binding partner. As the Sauerbrey equation establishes a linear relationship between mass and the recorded frequency variation signal, it is evident that quantitative analysis can be achieved directly from obtained experimental frequency variation data. Nevertheless, it is necessary to ensure that any parasitic signals that might arise from interferences are eliminated. In this regard, it is particularly important to determine the extent of acoustic losses (i.e. the resistive parameter) and their influence on the resulting resonant frequency values. The Martin equation (Equation 4) is the result of attempts to describe this relationship ($\Delta f_{visc}=-\Delta R/4\pi L_m$) theoretically [14]. On the other hand, it can be shown experimentally that the presence of charged species considerably modifies the resonance frequency [16,17,24,47,48]. An extension of the BVD equivalent circuit model, such as that presented in Figure 3a, has been suggested to include additional capacitance elements in parallel to account for such influence [24,48], and the frequency effect of charge addition can be quantified [24]. As the total frequency variation data are the sum of the mass contribution (Δf_{mass}), viscous contribution (Δf_{visc}) and charge contribution (Δf_{charge}), the mass contribution Δf_{mass} can thus be calculated and used in the Sauerbrey equation [24]. This approach has been used recently to estimate binding constants of anti-HIV-1 single chain antibodies and furthermore, to develop an anti-HIV1 immunosensor [7,18].

In contrast to the use of oscillator circuits and frequency counting, in which only frequency variation data can be obtained, and therefore only information about the deposited mass, the use of impedance analysis allows TSM sensor devices to be exploited to their full extent, because measurement of the dissipation of acoustic energy (as R_m, Q, or the dissipation factor $D=1/Q$) in addition to Δf, can increase significantly the information that can be gained from QCM experiments. In particular, when using impedance analysis, other properties of immobilized films (e.g. viscoelasticity or hydrophobicity), as well as their variation during the binding processes, can be monitored. As the acoustic impedance parameters are related to the properties of the propagation material (Table 2), it is possible to infer physical and structural information about the biological layers (e.g. DNA, proteins or cells) immobilized at the sensor surface. Such an approach can be used successfully to derive detailed information about the film thickness, shear viscosity, and elastic modulus of immobilized single- and double-stranded DNA [29], the hydration status of protein layers [49], and the conformational and structural modifications upon binding of a ligand to adsorbed proteins [7,50]. Additionally, combining classical theories of solution viscosity with acoustic measurements has also been shown to be highly effective in being able to distinguish quantitatively DNA molecules that have the same molecular mass but different structures, or to detect and predict DNA conformational changes that occur upon protein binding [51,52].

The ratio between ΔD *(or* ΔR_m*)* and Δf is a measure of the energy dissipation per surface-coupled unit mass, and thus specifically identifies the intrinsic properties of the immobilized biolayer. It has been used to derive additional information about the structure of the adsorbed layer, such as its relative rigidity or water content [53]. This ratio is gaining increasing importance to investigate cell adhesion to different types of surfaces [54–56], because its specificity can enable the identification of specific cell lines [57,58], or the specific state of the cell adhesion process [58,59]. This is because cell rigidity is related to the cytoskelton structure, which is characteristic for each cell type, and is reorganized during the process of cell adhesion.

Concluding remarks

QCMs have already proven to be efficient tools for the detection of molecules, for estimating affinity constants, and studying cell adhesion processes. Although the initial applications of QCM, which were based on the use of the Sauerbrey equation, have demonstrated the potential of QCM as a microweighing device, the observed frequency variations have been found to be influenced by several interferences, and have resulted in considerable deviations from conditions under which the Sauerbrey equation is valid. Recent studies have begun to take advantage of the physical principles that underlie these deviations, and have allowed QCM to become a more versatile tool that is able to sense a number of material-specific parameters of immobilized layers, such as their elastic moduli, surface charge densities, and viscosity. As changes in viscoelastic properties can be indicative of conformational changes that are not associated with adsorption or desorption of mass, ongoing QCM studies are now focusing on the possibility of deducing information regarding conformational change of proteins and DNA from the biosensing event, and on investigating different aspects of the biology of the cell, such as processes that involve cell adhesion, differentiation and stress responses.

When compared with other type of biosensors, particularly those based on SPR, the true power of piezoelectric sensors lies in the tremendous amount of information that can be obtained from measuring the acoustic impedance, thus opening the way for an increased array of potential applications, as additional properties of the immobilized biolayers in addition to its mass are obtained. On the other hand, piezoelectric sensors are currently not as sensitive as SPR sensors. The sensitivity of TSM depends on its thickness, which imposes mechanical constrains against building thinner and more sensitive sensors. This disadvantage will certainly be overcome in the near future as our knowledge increases about how to control and confine the propagation of surface acoustic waves, thus leading to the development of surface acoustic wave biosensors with significantly higher sensitivities.

Acknowledgments

The authors acknowledge funding from Fundação para a Ciência e a Tecnologia, projects PTDC/BIO/72307/2006 and PTDC/QUI/72631/2006, the grants SFHR/BPD/44895/2008 and SFHR/BD/35233/2007, and funding of the Associated laboratory IBB-Institute for Biotechnology and Bioengineering.

References

1 Cooper, M.A. and Singleton, V.T. (2007) A survey of the 2001 to 2005 quartz crystal microbalance biosensor literature: applications of acoustic physics to the analysis of biomolecular interactions. *J. Mol. Recognit.* 20, 154–184

2 Coté, G.L. (2003) Emerging biomedical sensing technologies and their applications. *IEEE sensors J.* 3, 251–266

3 Cavic, B.A. *et al.* (1999) Acoustic waves and the study of biochemical macromolecules and cells at the sensor-liquid interface. *The Analyst* 124, 1405–1420

4 Janshoff, A. *et al.* (2000) Piezoelectric mass-sensing devices as biosensors - An alternative to optical biosensors. *Angew Chem. Intern. Ed.* 39, 4004–4032

5 Etchenique, R. and Brudny, V.L. (2000) Characterization of porous thin films using quartz crystal shear resonators. *Langmuir* 16, 5064–5071

6 Fabreguette, F.H. *et al.* (2005) Quartz crystal microbalance study of tungsten atomic layer deposition using WF_6 and Si_2H_6. *Thin Solid Films* 488, 103–110

7 Ferreira, G.N.M. *et al.* (2007) Recombinant single-chain variable fragment and single domain antibody piezoimmunosensors for detection of HIV1 virion infectivity factor. *Biosens. Bioel.* 23, 384–392

8 Liu, Y. *et al.* (2004) Quartz crystal biosensor for real-time kinetic analysis of interaction between human TNF-α and monoclonal antibodies. *Sens. Actuators B* 99, 416–424

9 Modin, C. *et al.* (2006) QCM-D studies of attachment and differential spreading of pre-osteoblastic cells on Ta and Cr surfaces. *Biomaterials* 27, 1346–1354

10 Pan, W. *et al.* (1996) Kinetics of alkanethiol adsorption on gold. *Langmuir* 12, 4469–4473

11 Su, X-L. and Li, Y. (2005) A QCM immunosensor for *Salmonella* detection with simultaneous measurements of resonant frequency and motional resistance. *Biosens. Bioelectron.* 21, 840–848

12 McHale, G. and Newton, M. (2004) Surface roughness and interfacial slip condition for quartz crytal microbalances. *J. Appl. Phys.* 95, 373–380

13 Sauerbrey, G.Z. (1959) Use of quartz vibrator for weighing thin films on a microbalance. *Z. Phys.* 155, 206–222

14 Martin, S.J. *et al.* (1991) Characterization of a quartz crystal microbalance with simultaneous mass and liquid loading. *Anal. Chem.* 63, 2272–2281

15 Bandey, H. *et al.* (1999) Modeling the responses of thickness-shear mode resonators under various loading conditions. *Anal. Chem.* 71, 2205–2214

16 Kanazawa, K.K. and Gordon, J.G. (1985) The oscillation frequency of a quartz resonator in contact with liquid. *Anal. Chim. Acta* 175, 99–105

17 Kanazawa, K.K. (1997) Mechanical behaviour of films on the quartz microbalance. *Faraday Discuss.* 107, 77–90

18 Encarnação, J.M. *et al.* (2007) Piezoelectric biosensors for biorecognition analysis: Application to the kinetic study of HIV-1 Vif protein binding to recombinant antibodies. *J. Biotechnol.* 132, 142–148

19 Beck, R. *et al.* (1992) Influence of the surface microstructure on the coupling between a quartz oscillator and a liquid. *J. Electrochem. Soc.* 139, 453–461

20 Daikhin, L. *et al.* (2002) Influence of roughness on the admittance of the quartz crystal microbalance immersed in liquids. *Anal. Chem.* 74, 554–561

21 Rodahl, M. *et al.* (1996) QCM operation in liquids: an explanation of measured variations in frequency and *Q* factor with liquid conductivity. *Anal. Chem.* 68, 2219–2227

22 Etchenique, R. and Buhse, T. (2000) Anomalous behaviour of the quartz crystal microbalance in the presence of electrolytes. *The Analyst* 125, 785–787

23 Etchenique, R. and Buhse, T. (2002) Viscoelasticiy of the diffuse electric double layer. *The Analyst* 127, 1347–1352

24 Encarnação, J.M. *et al.* (2007) Influence of electrolytes in the QCM response: discrimination and quantification of the interference to correct microgravimetric data. *Biosens. Bioelectron.* 22, 1351–1358

25 Granstaff, V.E. and Martin, S.J. (1994) Characterization of a thickness-shear mode quartz resonator with multiple nonpiezoelectric layers. *J. Appl. Phys.* 75, 1319–1329

26 Bandey, H.L. *et al.* (1997) Viscoelastic characterization of electroactive polymer films at the electrode/solution interface. *Faraday Discuss.* 107, 105–121

27 Lucklum, R. and Hauptmann, P. (2000) The $\Delta f - \Delta R$ QCM technique: an approach to an advanced sensor signal interpretation. *Electrochim. Acta* 45, 3907–3916

28 Rodahl, M. *et al.* (1997) Simultaneous frequency and dissipation factor QCM measurements of biomolecular adsorption and cell adhesion. *Faraday Discuss.* 107, 229–246

29 Voinova, M. *et al.* (1999) Viscoelastic acoustic response of layered polymer films at fluid–solid interfaces: continuum mechanics approach. *Phys. Scripta.* 59, 391–396

30 Larsson, C. *et al.* (2003) Characterization of DNA immobilization and subsequent hybridization on a 2D arrangement of streptavidin on a biotin-modified lipid bilayer supported on SiO_2. *Anal. Chem.* 75, 5080–5087

31 Nunalee, F.N. and Shull, K.R. (2006) Quartz crystal microbalance studies of polymer gels and solutions in liquid environments. *Anal. Chem.* 78, 1158–1166

32 Daikhin, L. and Urbakh, M. (1997) Interaction of surface acoustic waves with viscous liquids. *Faraday Discuss.* 107, 27–38

33 Martin, S.J. *et al.* (1993) Effect of surface roughness on the response of thickness-shear mode resonators in liquids. *Anal. Chem.* 65, 2910–2922

34 Cavic, B.A. *et al.* (1997) Acoustic waves and the real-time study of biochemical macromolecules at the liquid/solid interface. *Faraday Discuss.* 107, 159–176

35 Hayward, G.L. and Thompson, M. (1998) A transverse shear model of a piezoelectric chemical sensor. *J. Appl. Phys.* 83, 2194–2201

36 Shana, Z.A. and Josse, F. (1994) Quartz crystal resonators as sensors in liquids using the acoustoelectric effect. *Anal. Chem.* 66, 1955–1964

37 Martin, B.A. and Hager, H.E. (1989) Velocity profile on quartz crystals oscillating in liquids. *J. Appl. Phys.* 65, 2630–2635

38 Bouche-Pillon, D. *et al.* (1995) Validation of the quartz-crystal microbalance response in liquid for sensor applications. *Sens. Actuators B* 24, 257–259

39 Etchenique, R. and Weisz, A.D. (1999) Simultaneous determination of the mechanical moduli and mass of thin layers using nonadditive quartz crystal acoustic impedance. *J. App. Physics* 4, 1994–2000

40 Lucklum, R. and Hauptmann, P. (2000) The quartz crystal microbalance: mass sensitivity, viscoelasticity and acoustic amplification. *Sens. Actuators B* 70, 30–36

41 Zhou, A. *et al.* (2000) Impedance analysis for the investigation of the behaviors of piezoelectric quartz crystal in the liquid at harmonic resonance. *Sens. Actuators B* 67, 68–75

42 Sabot, A. and Krause, S. (2002) Simultaneous quartz crystal microbalance impedance and electrochemical impedance measurements. Investigation into the degradation of thin polymer films. *Anal. Chem.* 74, 3304–3311

43 Auge, J. *et al.* (1995) New design for QCM sensors in liquids. *Sens. Actuators B* 24, 43–48

44 Yang, M. and Thompson, M. (1993) Multiple chemical information from the thickness mode acoustic wave sensor in the liquid phase. *Anal. Chem.* 65, 1158–1168

45 Bizet, K. *et al.* (1998) Validation of antibody-based recognition by piezoelectric transducers through electroacoustic admittance analysis. *Biosens. Bioelectron.* 13, 259–269

46 Ha, T.H. and Kim, K. (2001) Adsorption of lipid vesicles on hydrophobic surface investigated by quartz crystal microbalance. *Langmuir* 17, 1999–2007

47 Ghafouri, S. and Thompson, M. (2000) Interfacial properties and the response of the transverse acoustic wave device in electrolytes. *Electroanalysis* 12, 326–336

48 Ghafouri, S. and Thompson, M. (2001) Electrode modification and the response of the acoustic shear wave device operating in liquid. *Analyst* 126, 2159–2167

49 Ozeky, T. *et al.* (2007) Hydration and energy dissipation measurements of biomolecules on a piezoelectric quartz oscillator by admittance analyses. *Anal. Chem.* 79, 79–88

50 Wang, X. *et al.* (2006) Conformational chemistry of surface-attached calmodulin detected by acoustic shear propagation. *Mol. Biosyst.* 2, 184–192

51 Tsortos, A. *et al.* (2008) Quantitative determination of size and shape of surface-bound DNA using an acoustic wave sensor. *Biophys. J.* 94, 2706–2715

52 Tsortos, A. *et al.* (2008) Shear acoustic wave biosensor for detecting DNA intrinsic viscosity and conformation: A study with QCM-D. *Biosens. Bioelectron.* 24, 836–841
53 Hook, F. *et al.* (2001) Variations in coupled water, viscoelastic properties, and film thickness of a mefp-1 protein film during adsorption and cross-linking: a quartz crystal microbalance with dissipation monitoring, ellipsometry, and surface plasmon resonance study. *Anal. Chem.* 73, 5796–5804
54 Fohlerová, Z. *et al.* (2007) Adhesion of eukaryotic cell lines on the gold surface modified with extracellular matrix proteins monitored by the piezoelectric sensor. *Biosens. Bioelectron.* 22, 1896–1901
55 Guo, M. *et al.* (2008) Enhanced adhesion/spreading and proliferation of mammalian cells on electropolymerized porphyrin film for biosensing applications. *Biosens. Bioelectron.* 23, 865–871
56 Khraiche, M.L. *et al.* (2005) Acoustic sensor for monitoring adhesion of Neuro-2A cells in real-time. *J. Neurosci. Meth.* 144, 1–10
57 Pax, M. *et al.* (2005) Measurment of fast fluctuation of viscoelastic properties with the quartz crystal microbalance. *Analyst* 130, 1474–1477
58 Wang, X. *et al.* (2008) Surface immobilization and properties of smooth muscle cells monitored by on-line acoustic wave detector. *Analyst* 133, 85–92
59 Li, F. *et al.* (2007) Monitoring cell adhesion by using thickness shear mode acoustic wave sensors. *Biosens. Bioelectron.* 23, 42–50